# Bu-Shen-Ning-Xin decoction suppresses osteoclastogenesis by modulating RANKL/OPG imbalance in the CD4+ T lymphocytes of ovariectomized mice

JIA-LI ZHANG[1-3], XUE-MIN QIU[1-3], NA ZHANG[1-3], WEI TANG[4], HANS-JÜRGEN GOBER[5], DA-JIN LI[1,2] and LING WANG[1-3]

[1]Laboratory for Reproductive Immunology, Hospital and Institute of Obstetrics and Gynecology, IBS, Fudan University Shanghai Medical College; [2]The Academy of Integrative Medicine, Fudan University; [3]Shanghai Key Laboratory of Female Reproductive Endocrine Related Diseases, Obstetrics and Gynecology Hospital of Fudan University, Shanghai 200011, P.R. China; [4]Hepato-Biliary-Pancreatic Surgery Division, Department of Surgery, Graduate School of Medicine, University of Tokyo, Tokyo 113-8655, Japan; [5]Department of Pharmacy, Neuromed Campus, Johannes Kepler University, 4020 Linz, Austria

Received May 12, 2016; Accepted March 22, 2018

DOI: 10.3892/ijmm.2018.3645

**Abstract.** Postmenopausal osteoporosis (PMO) has been recognized as an inflammatory condition. CD4+ T cells serve a key role in the interaction between bone metabolism and the immune system. Bu-Shen-Ning-Xin decoction (BSNXD), a traditional Chinese medicine, has been ultilized as a remedy for PMO. In the present study, the aim was to investigate the immune modulatory effects of BSNXD on CD4+ T cells, receptor activation of nuclear factor κB ligand (RANKL)/osteoprotegerin (OPG) imbalance, skeletal parameters and osteoclastogenesis. Ovariectomized (OVX) mice were treated with a series of concentrations of BSNXD and then autopsied. The bone phenotype was analyzed by micro computed tomography. CD4+ T cells were isolated and their percentage was measured using flow cytometry (FCM). RANKL and OPG expression by the CD4+ T cells at the transcriptional and translational levels were quantified by reverse transcription-quantitative polymerase chain reaction, ELISA and FCM. CD4+ T cells were cultured with blood serum derived from BSNXD-treated OVX mice (BSNXD-derived serum) and the apoptosis rate was quantified by FCM. CD4+ T cells were co-cultured with bone marrow-derived macrophages and exposed to BSNXD-derived serum to whether CD4+ T cells are involved in BSNXD-modulated osteoclastogenesis and the results were quantified via tartrate-resistant acid phosphatase staining. The results revealed that BSNXD ameliorated OVX-induced bone loss, prevented the expansion of CD4+ T cells and restored the RANKL/OPG imbalance in the CD4+ T cells of OVX mice. *In vitro*, BSNXD-derived serum promoted the apoptosis of CD4+ T cells. The co-culture system demonstrated that CD4+ T cells from OVX mice increase osteoclastogenesis, while this effect was suppressed by BSNXD administration. The findings of the study collectively suggest that BSNXD exerts an immunoprotective effect on the bone phenotype of OVX mice by ameliorating RANKL/OPG imbalance in CD4+ T cells and attenuating osteoclastogenesis.

*Correspondence to:* Dr Ling Wang, Laboratory for Reproductive Immunology, Hospital and Institute of Obstetrics and Gynecology, IBS, Fudan University Shanghai Medical College, 413 Zhaozhou Road, Shanghai 200011, P.R. China
E-mail: dr.wangling@fudan.edu.cn

*Key words:* herbal formula, osteoimmunology, osteoclast, RANKL, postmenopausal osteoporosis, reproductive-endocrine-immune metabolic network

## Introduction

Postmenopausal osteoporosis (PMO) is a major health problem for women, and is characterized by reduced bone mineral density (BMD) following the menopause, leading to raised bone remodeling rates and increased skeletal fragility risk (1,2). These changes are mainly caused by declining ovarian function, which results in sex hormone disorders and an imbalance between osteoblast-mediated bone formation and osteoclast (OC)-mediated bone resorption (3). OCs are derived from hematopoietic stem cells via a process driven by two key factors: Macrophage-colony-stimulating factor (M-CSF) and receptor activation of nuclear factor κB ligand (RANKL). RANKL is able to activate a variety of downstream signaling pathways required for OC development, resulting in increased osteoclastogenesis and accelerated bone loss (4-6). Osteoprotegerin (OPG), which belongs to the tumor necrosis factor receptor superfamily, is a secreted glycoprotein that has been demonstrated to be associated with reductions in osteoclastogenesis and OC activity in rats, and therefore may be a protective factor against bone loss in osteoporosis (7,8). Thus, the balance between RANKL/OPG may modulate osteoclastogenesis.

PMO is a state of bone inflammation and sex steroid deficiency (9,10). Sex steroids have regulatory functions on the

immune system, including T lymphocytes. Previous studies have demonstrated that descending levels of estrogen following the menopause are associated with increased bone inflammation, in addition to enhanced osteoclastogenesis and bone resorption (11,12). In ovariectomized (OVX) mice, an animal model in which ovarian hormones are depleted via ovariectomy, an increase in the proliferation of activated T cells has been observed, which resulted in an expansion of the T cell pool in the bone marrow (BM) (13). Furthermore, several subsets of T lymphocytes, including cluster of differentiation (CD)4+ T cells, have been shown to be increased in the peripheral blood of osteoporotic patients (14). RANKL may serve a pivotal role in inflammation-mediated bone loss; activated T cells are able to express high levels of RANKL and directly induce OC differentiation by acting on OC precursor cells (15-20).

The treatments currently available for PMO are limited. Estrogen replacement therapy has been used to ameliorate menopausal symptoms for women; however, it is limited due to its adverse effects on the uterus, breasts and cardiovascular system. In addition, the critical window hypothesis of hormone therapy has been suggested (21). Studies have indicated that early estrogen replacement therapy, usually started in women <60 years old and/or <10 years postmenopause, is more effective than that in other women (22,23). Selective estrogen receptor modulators, such as raloxifene, have an estrogen agonist effect in bone, while they exert an antiestrogenic effect in the uterus and breast and increase the risk for venous thromboembolic events. Bisphosphonates are considered to inactivate OCs and to decrease bone resorption; however, the reversal of their antiresorptive effect is delayed following discontinuation due to their long elimination half-life (24). Denosumab, the human monoclonal immunoglobulin G (IgG) antibody to RANKL, has been demonstrated to be efficacious in reducing fracture incidence, while its safety remains unclear (25,26). Teriparatide is the only anabolic agent with ability to increase BMD; however, this advantage is not observed in all patients (27).

Bu-Shen-Ning-Xin decoction (BSNXD) is a traditional Chinese medicine (TCM) that has been used for hundreds of years to prevent menopause- and aging-associated disorders (28). Unlike modern medicine which is target-oriented, herbal TCMs are usually composed of several individual herbs to form a specific formulation that has good therapeutic efficacy and few adverse effects (29). BSNXD is composed of dried Rehmannia root, common Anemarrhena rhizome, bark of Chinese Corktree, Barbary Wolfberry fruit, Chinese Dodder seed, Shorthorned Epimedium herb, Spina date seed and Oriental water plantain rhizome. These herbs are mixed together in specific quantities and proportions (Table I), to keep the phytochemical components as constant as possible and to maximize their pharmacological effect (30) BSNXD has been demonstrated to have beneficial effects on bone metabolism in PMO (30), but the molecular mechanism of that effect remains unclear. A previous study identified 16 molecular components in a BSNXD fingerprint analysis, including acteoside, berberine, jatrorrizine and icariin (30). In other studies, BSNXD ameliorated the loss of BMD and bone volume (BV) in OVX mice without affecting the serum estrogen concentration or uterus, suggesting that it may act as a regulator for the endocrine and immune systems and inhibit osteoclastogenesis by abrogation of RANKL-induced signaling pathways and by increasing the level of dehydroepiandrosterone (30,31).

In recent years, a growing number of studies has found that TCMs have immunomodulatory effect (32,33). The aim of the present study was to further explore the efficacy and mechanism of BSNXD as a potential osteoimmunological regulator in the therapy of PMO. *In vivo*, the effects of BSNXD administration on OVX-induced CD4+ T-cell proliferation and the expression of RANKL and OPG were investigated, and its immunomodulatory effects on osteoclastgenesis and skeletal parameters were evaluated. *In vitro*, co-cultures of CD4+ T cells with BM macrophages (BMMs) were exposed to different concentrations of blood serum isolated from BSNXD-treated OVX mice. The aim of the present study was to probe into whether CD4+ T cells are involved in BSNXD-modulated osteoclastgenesis and responsible for the improvement of bone morphometric parameters in OVX mice.

## Materials and methods

*Reagents and chemicals*. Complete RPMI-1640 medium used for the culture of mouse lymphocytes from BM and spleen was purchased from Wisent Inc. (St. Bruno, QC, Canada), and was supplemented with 10% fetal bovine serum (FBS), penicillin (100 U/ml) and streptomycin (100 $\mu$g/ml). Enzyme-linked immunosorbent assay (ELISA) kits for soluble RANKL (sRANKL; MTR00) were purchased from R&D Systems, Inc. (Minneapolis, MN, USA). ELISA kits for OPG (E108Mu) were purchased from USCN Life Sciences, Inc. (Wuhan, China). Leukocyte Acid Phosphatase kits were purchased from Sigma-Aldrich (Merck KGaA, Darmstadt, Germany). Anti-CD28 (14-0281-86) and anti-RANKL (MA1-41019) antibodies were obtained from eBioscience (Thermo Fisher Scientific, Inc., Waltham, MA, USA). Fluorescein isothiocyanate (FITC)-conjugated anti-mouse CD3 (555274), phycoerythrin (PE)-conjugated anti-mouse CD4 (553048) and PE-CY™5-conjugated anti-mouse CD8a (553034) antibodies were purchased from BD Biosciences (San Jose, CA, USA). TRIzol was purchased from Thermo Fisher Scientific, Inc. Transcriptor First Strand cDNA synthesis kit and oligo primers were purchased from (Roche Molecular Systems, Inc., Branchburg, NJ, USA). SYBR Green Master Mix used for quantitative polymerase chain reaction (qPCR) was obtained from Applied Biosystems (Thermo Fisher Scientific, Inc.).

*Preparation of BSNXD extracts*. The herbal fomula BSNXD was obtained from the pharmacy of the Hospital of Obstetrics and Gynecology, Fudan University (Shanghai, China) and consisted of eight crude herbs as listed in Table I. It was formulated in line with TCM theory and the clinical experience of the present research team. These products were made with good manufacturing practice at the Institute of Obstetrics and Gynecology, Fudan University Shanghai Medical College. The eight crude herbs powder of BSNXD was prepared according to the Chinese Pharmacopoeia 2005 (34,35). Crude water extracts were prepared from powdered BSNXD (34,35). The fingerprint analysis of BSNXD has been conducted previously in a previous study (30).

*Mice*. Inbred strains of BALB/c mice (age, 10-12 weeks) were obtained from Jackson Laboratory (Ben Harbor, ME, USA) and subsequently maintained in the Laboratory Animal Facility of Chinese Academy of Sciences (Shanghai, China).

Table I. Composition and preparation of the herbal formula Bu-Shen-Ning-Xin decoction.

| Crude herbs | Latin names | Content (g) | Percentage | Main components |
|---|---|---|---|---|
| Dried Rehmannia root | *Radix Rehmanniae* Exsiccata | 15 | 15.2 | Catalpol<br>Acteoside<br>Apigenin |
| Common Anemarrhena rhizome | *Anemarrhena osphodeloides* Bunge | 15 | 15.2 | Sarsasapogenin<br>Timosaponin<br>Markogenin |
| Bark of Chinese Corktree | *Phellodendron amurense* Rupr. | 9 | 9.1 | Berberine<br>Phellodendrine<br>Jatrorrhizine |
| Barbary Wolfberry fruit | *Lycium barbarum* | 15 | 15.2 | *Lycium barbarun* polysaccharides<br>β-carotene<br>Quercetin |
| Chinese Dodder seed | *Cuscuta chinensis* | 12 | 12.1 | Quercetin<br>Kaempferol<br>Hyperoside |
| Shorthorned Epimedium herb | *Epimediun brevicornum* Maxim | 12 | 12.1 | Icariin<br>Icariin I<br>Icariin II |
| Spina date seed | *Ziziphus jujube* Mill. var. *spinosa* | 9 | 9.1 | Jujuboside A<br>Jujuboside A1<br>Jujuboside C |
| Oriental water plantain rhizome | *Alisma plantago-aquatica* Linn. | 12 | 12.1 | Alisol A<br>Alisol B<br>Alisol C 23 acetate |

Mice were habituated to the housing conditions under a strict 12-h light/dark cycle at 22˚C for 2 days with a humidity controlled between 40 and 70%. Normal chow diet and water were provided *ad libitum*.

*Generation of the PMO mouse model and drug administration*. The animal experiments were performed according to the Principles of Laboratory Animal Care of the Department of Laboratory Animal Science, Fudan University and approved by the Ethics Committee of Fudan University. We filtrated 35 female BALB/c mice, 8 weeks old, with a body mass of 20-30 g. Following the bilateral oophorectomy of 30 mice, 5 mice died as a result of the surgery and were excluded from the analysis, and there were no deaths from other causes. The surviving mice were randomly divided into five groups (each n=5) as follows: OVX; OVX + BSNXD low dose; OVX + BSNXD mid dose; OVX + BSNXD high dose and OVX + estradiol (E2). A sham group (5 mice) underwent the surgical procedure without ovariectomy.

The OVX control group was treated with saline and the OVX + BSNXD low dose, OVX + BSNXD mid dose and OVX + BSNXD high dose groups were treated twice daily with 0.5 ml concentrated BSNXD extract (total raw herb contents 0.5, 1 and 2 g/ml, respectively, w/v) by oral administration (Table I) at dosages that were 4.5-, 9- and 18-fold the human adult dose, based on an established formula for human-mice drug conversion (30). The OVX + E2 group received E2 treatment (100 $\mu$g/kg/day orally) (31,36,37).

Following drug administration for 8 weeks, all animals were autopsied. The serum of the animals was collected for ELISA. The distal femurs of the mice were dissected for static and dynamic histomorphometric analysis. Bones and spleens were collected in PBS. The BM was flushed out and total lymphocytes were isolated from the BM by means of density gradient centrifugation using Hisep LSM 1084 (1.084±0.0010 g/ml; HiMedia Laboratories, Mumbai, India) and then labelled with fluorescent antibodies for the analysis of $CD4^+$ T cells. Splenic and BM mononuclear cells were collected to examine the percentage of $CD4^+$ T cells and the alteration of RANKL/OPG expression in $CD4^+$ T cells by fluorescence activated cell sorting (FACS), reverse transcription (RT)-qPCR analysis and ELISA.

*Bone phenotype analysis*. The micro-architecture of the distal femurs of the mice was analyzed using micro-computed tomography (ScanXmate-A100S Scanner; Comscan Techno Co., Kanagawa, Japan). Three-dimensional (3D) microstructural image data were reconstructed and structural parameters were calculated using 3D trabecular bone analysis software (TRI/3D-BON; Ratoc System Engineering, Co., Ltd., Tokyo, Japan), including BV/tissue volume (TV) ratio, trabecular number, trabecular thickness and trabecular plate separation.

Table II. Sequences of qPCR primers.

| Gene name | Primer sequence | Accession no. |
|---|---|---|
| RANKL | P1: 5'-TGAAGACACACTACCTGACTCCTG-3'<br>P2: 5'-CCACAATGTGTTGCAGTTCC-3' | AF019048.1 |
| OPG | P1: 5'-GTTTCCCGAAGGACCACAAT-3'<br>P2: 5'-CCATTCAATGATGTCCAGGAG-3' | U94331.1 |
| GAPDH | P1: 5'-AGCTTGTCATCAACGGGAAG-3'<br>P2: 5'-TTTGATGTTAGTGGGGTCTCG-3' | NM_008084.2 |

qPCR, quantitative polymerase chain reaction; RANKL, receptor activation of nuclear factor κB ligand; OPG, osteoprotegerin.

*Isolation of CD4+ T cells from murine spleen or BM*. Single cell suspensions were obtained from the spleen or BM and incubated with magnetic beads coated with anti-mouse CD4 antibody (Miltenyi Biotec, Inc., Auburn, CA, USA). CD4+ T cells were isolated in strict accordance with the manufacturer's protocol (38). These purified cells were then collected in TRIzol for RT-qPCR analysis.

*RT-qPCR*. Total RNA was extracted from isolated CD4+ T cells using TRIzol. cDNA was synthesized from 1 $\mu$g total RNA with the Transcriptor first strand cDNA synthesis kit (04379012001; Roche Molecular Systems, Inc.; synthesis at 55˚C for 30 min and inactivation at 85˚C for 5 min). SYBR Green Master mix was used for quantitative determination of the mRNAs for OPG, RANKL and GAPDH in a 20-$\mu$l reaction system following an optimized protocol. The target mRNA expression was normalized using the expression levels of GAPDH. We used the $2^{-\Delta\Delta Cq}$ method for mRNA quantification (39). qPCR was performed using the following conditions: 95˚C for 5 min; 40 cycles of denaturation at 94˚C for 2 min and annealing and extension at 62˚C for 30 sec; and extension at 72˚C for 30 sec. The primers used for each gene are presented in Table II.

*Flow cytometry (FCM)*. Mononuclear cells from the BM/spleen were labelled with anti-CD3, CD4 and CD8a antibodies, namely FITC-conjugated anti-mouse CD3, PE-conjugated anti-mouse CD4, PE-CY5-conjugated anti-mouse CD8a antibodies, to assess the CD4+ precentages of CD3+ cells. The specificity of immunostaining was ascertained by the background fluorescence of cells incubated with IgG isotype controls. Fluorescence data from ≥10,000 cells were collected from each sample. Immunostaining was performed according to the manufacturer's protocol. FACSCalibur and FACSAria flow cytometers (BD Biosciences) were used to quantify the CD4+ percentages of CD3+ cells in all the groups. CellQuest™ software (BD Biosciences) was used to analyze the flow cytometry data.

*Evaluation of RANKL expression on the cell surface of CD4+ T cells*. CD4+ T cells were purified from mouse splenocytes using a magnetic cell sorting system as described above. These cells were cultured in RPMI-1640 medium supplemented with 10% FBS, penicillin (100 U/ml) and streptomycin (100 $\mu$g/ml). CD4+ T cells ($5x10^5$ cells/ml) were activated with plate-coated anti-CD3 (2 $\mu$g/ml; MA5-17655; Thermo Fisher Scientific, Inc.) and anti-CD28 (0.5 $\mu$g/ml). Activated T cells were treated with anti-RANKL antibody or control rat IgG (02-9602; Thermo Fisher Scientific, Inc.), followed by anti-mouse IgG-phycoerythrin (PE; PA5-33283). The cells were then analyzed for cell surface RANKL expression via FACS using a FACSCalibur flow cytometer.

*Evaluation of sRANKL and OPG production by CD4+ T cells*. The concentrations of sRANKL and OPG in the culture supernatants were measured using the aforementioned ELISA kits according to the manufacturers' protocol.

*Modulatory effect of BSNXD on CD4+ T cells in vitro*. CD4+ T cells obtained from the spleen of OVX mice were cultured in RMPI-1640 medium supplemented with 10% fetal calf serum (FCS; SH30073.02; HyClone; GE Healthcare Life Science, Pittsburgh, PA, USA) for 3 days. To estimate the effect of BSNXD on the apoptosis rate of CD4+ T cells, the cells were exposed to 20% OVX mouse serum as control, serial concentrations (10, 15 and 20%) of OVX + mid-dose BSNXD group-derived serum or OVX + E2 group-derived serum (containing 10 nM 17β-E2). Following incubation for 72 h, the apoptosis rate of the CD4+ T cells was measured by FCM.

*Apoptosis analysis of CD4+ T cells by FCM*. After incubation for 72 h, the CD4+ T cells were washed with PBS and the apoptotic cells were stained using an Annexin V-FITC/PI dual-labeling technique (Annexin V-FITC/PI Apoptosis detection kit; RC201-50; RainBio) and analyzed by FCM. The quantity of Annexin V-FITC+/PI- cells corresponded to early apoptosis. In every sample, $1x10^5$ cells were counted. The experiment was repeated five times.

*Modulatory effect of BSNXD on CD4+ T cells co-cultured with BMMs in vitro*. To investigate whether CD4+ T cells are involved in BSNXD-modulated osteoclastogenesis, BMMs from the femurs and tibias of OVX mice were co-cultured with CD4+ T cells ($5x10^6$/ml) from OVX mice in RPMI-1640 medium supplemented with 10% FCS and 10 ng/ml M-CSF for 2 days and then exposed to RANKL for stimulation and 20% serum of OVX mice, 20% serum of mid-dose BSNXD treated OVX mice, or OVX + E2 group-derived serum (containing 10 nM 17β-E2) for 3 days. BMMs cultured with 20% serum of OVX mice served as a negative control. Osteoclastogenesis was evaluated with tartrate-resistant acid phosphatase (TRAP) staining by means of the Leukocyte Acid Phosphatase kit. TRAP-positive

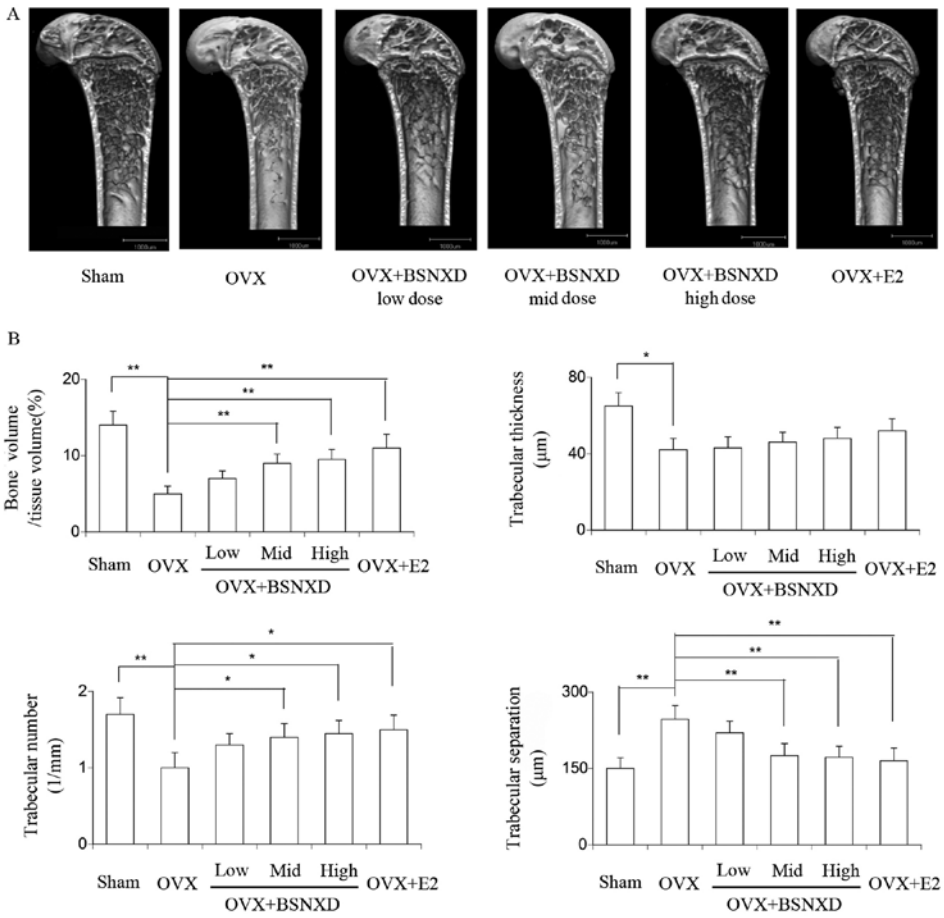


Figure 1. Effect of BSNXD on the bone phenotype of the mice. The OVX mice were randomly divided into the following groups: OVX control group treated with saline (n=5); OVX + BSNXD low-, mid- and high-dose groups treated with 0.5 ml evaporated BSNXD extract, twice daily (total raw herbs 0.5, 1 and 2 g/ml, w/v) by oral administration (n=5 per group); and the OVX + E2 group treated with E2 (100 $\mu$g/kg/day orally; n=5). After 8 weeks of treatment, all mice were sacrificed following the final treatment and bone tissues were harvested for further investigation. Micro-computed tomography was performed to analyze the bones of the mice in each group. (A) Micro-computed tomography images. (B) Bone volume/tissue volume (%), trabecular thickness ($\mu$m), trabecular number (1/mm) and trabecular separation ($\mu$m) were measured. Data are expressed as the mean ± standard error of the mean. $^{**}$P<0.01 and $^{*}$P<0.05 as indicated. BSNXD, Bu-Shen-Ning-Xin Decoction; OVX, ovariectomized; E2, estradiol.

MNCs (≥5 nuclei) were counted using a microscope (31). Results from four independent experiments are shown.

*Statistical analysis*. All values are expressed as the mean ± standard error of the mean. Data were analyzed using SPSS 19.0 software (IBM Corp., Armonk, NY, USA) and differences were evaluated by one-way analysis of variance followed by Bonferroni post hoc test. P<0.05 was considered to indicate a statistically significant difference.

## Results

*Effect of BSNXD administration on the bone phenotype of OVX mice*. In the mice, ovariectomy disrupted the balance between bone resorption and formation in favor of resorption, resulting in the loss of bone microarchitecture in the OVX group compared with the sham group. Analysis of the femurs of the mice in the OVX group by micro-computed tomography revealed a significant reduction in BV/TV ratio, trabecular numbers and trabecular thickness, and a significant increase in trabecular separation (P<0.05 vs. sham; Fig. 1). Following treatment for 8 weeks with E2, or low-, mid- or high-dose BSNXD, the loss of BV and changes in bone microarchitecture were ameliorated or prevented compared with that in the OVX group. A significant reduction of trabecular separation was observed in the treated mice (P<0.05 vs. OVX; Fig. 1A and B), while no significant difference was detected in trabecular thickness (Fig. 1B).

*OVX-induced expansion of CD4$^+$ T cells is attenuated by the administration of mid-dose BSNXD*. PMO is a result of chronic inflammation due to sex hormone deficiency, which is closely associated with OC function. The proportions of CD4$^+$ T cells in the BM and spleen were analyzed using FCM. In the OVX group, the BM and spleen exhibited a significant increase in the proportion of CD4$^+$ T cells compared with the sham group (P<0.01; Fig. 2), which is in accordance with a previous study (40). Administration of BSNXD for 8 weeks normalized the percentage of CD4$^+$ T cells in the spleen and BM of OVX mice significantly in the mid-dose group, with the same efficacy as treatment with E2. However, no significant effect was observed in the low- and high-dose BSNXD groups (Fig. 2B).

*BSNXD modulates the RANKL/OPG balance of CD4$^+$ T cell in OVX mice*. To determine the RANKL/OPG ratio of the CD4$^+$

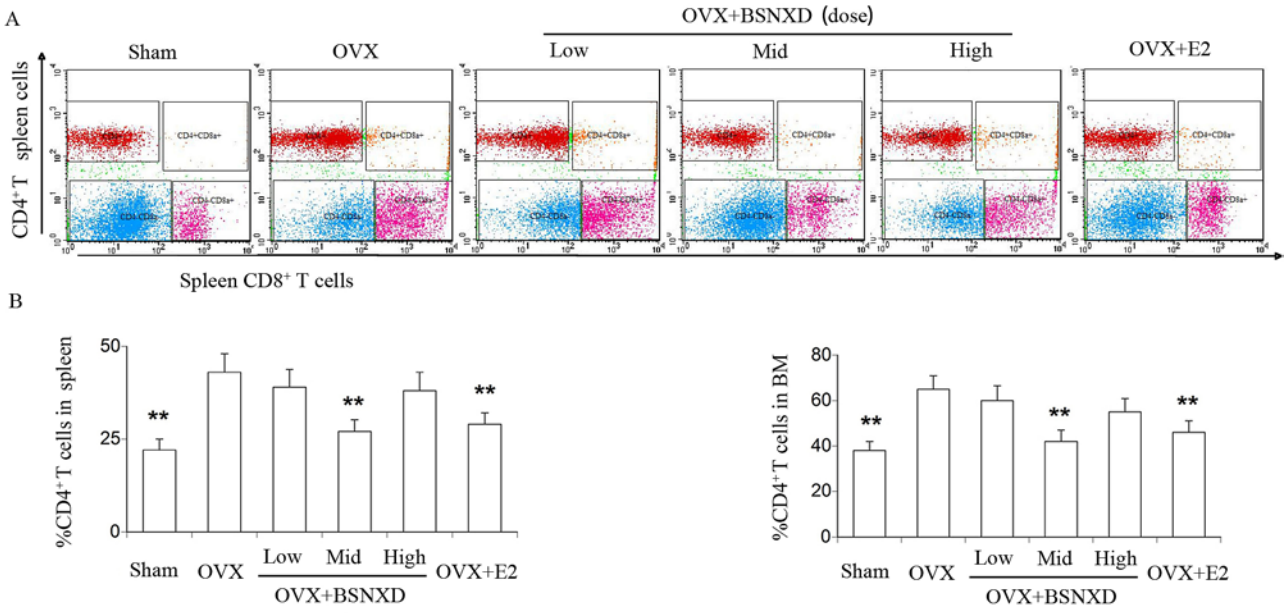


Figure 2. Mid-dose BSNXD administration significantly inhibited the OVX-induced increases of CD4+ T cells in the spleen and BM. Following 8 weeks of BSNXD administration, mice in the six experimental groups were sacrificed. The BM was then flushed out and single cells were isolated from the spleen by means of density (1,084±0,0010 g/ml) gradient centrifugation and then labelled with fluorescent antibodies to examine the percentage of CD4+ T cells using flow cytometry. (A) Images of the quantification of CD4+ T cells in the spleen in each group by flow cytometry. (B) Percentage of CD4+ T cells in the spleen or BM. Data are expressed as the mean ± standard error of the mean. **P<0.01 vs. OVX. BSNXD, Bu-Shen-Ning-Xin Decoction; OVX, ovariectomized; E2, estradiol; BM, bone marrow; CD, cluster of differentiation.

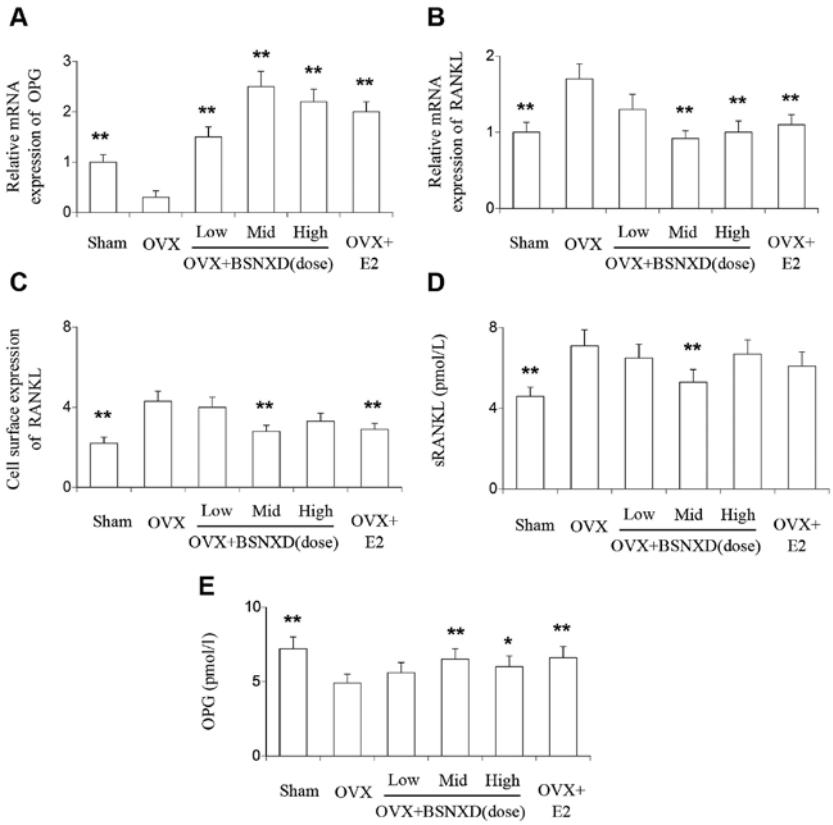


Figure 3. Modulatory effect of BSNXD on RANKL and OPG. Following 8 weeks of BSNXD administration, mice in six experimental groups were sacrificed, and single cells were isolated from the spleen by means of density gradient centrifugation. CD4+ T cells were isolated from single cells via magnetic bead selection. The CD4+ T cells were separated into three portions for testing. One portion was used to estimate the relative mRNA expression of RANKL and OPG by reverse transcription-quantitative polymerase chain reaction, another was used to determine the cell surface expression of RANKL by flow cytometry, and the third was cultured *in vitro* and the supernatant harvested to detect the sRANKL and OPG levels by ELISA. (A) Relative mRNA expression of RANKL, (B) relative mRNA expression of OPG and (C) cell surface expression of RANKL. Protein levels of (D) RANKL and (E) OPG in the cell culture supernatant. Data are expressed as the mean ± standard error of the mean. **P<0.01 and *P<0.05 vs. OVX. BSNXD, Bu-Shen-Ning-Xin Decoction; OVX, ovariectomized; E2, estradiol; RANKL, receptor activation of nuclear factor κB ligand; sRANKL, soluble RABKL; OPG, osteoprotegerin; CD, cluster of differentiation.

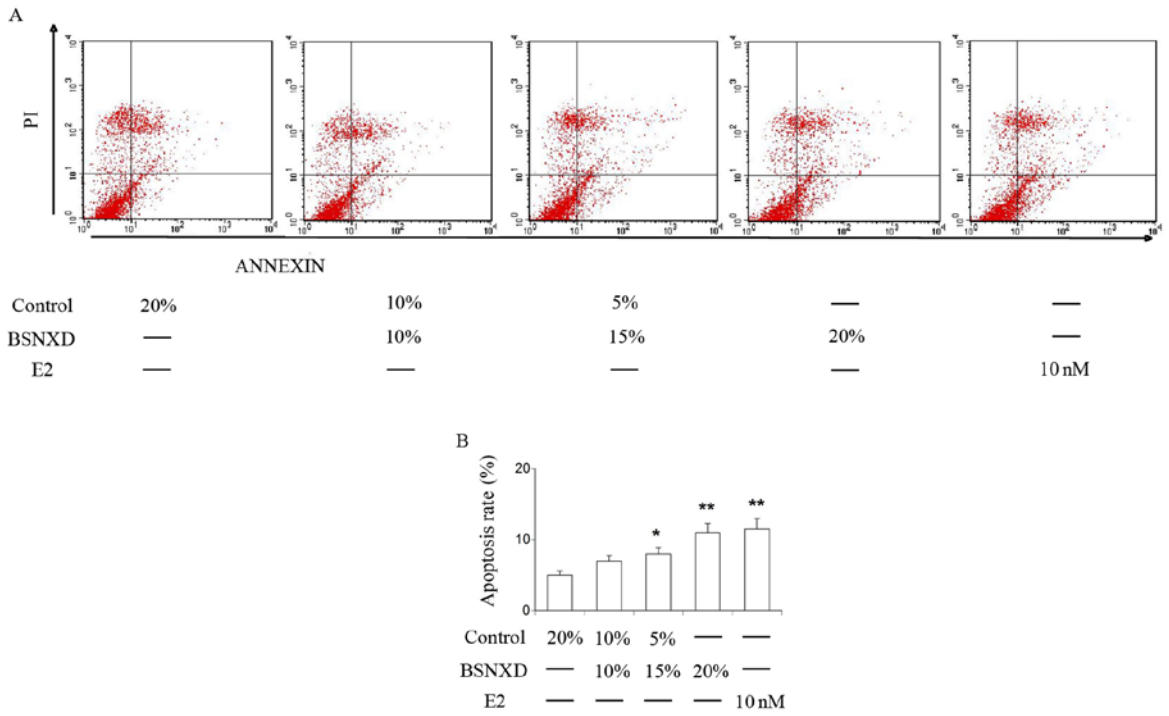


Figure 4. Effect of mid-dose BSNXD on the apoptosis rate of CD4+ T cells *in vitro*. CD4+ T cells were isolated from the spleen of OVX mice and then exposed to serial concentrations (10, 15 and 20%) of OVX + mid-dose BSNXD group-derived serum or OVX + E2 group-derived serum (containing 10 nM 17β-E2). Following incubation for 72 h, the apoptosis rate of the CD4+ T cells was measured using FCM. (A) Images showing the detection of apoptosis of CD4+ T cells from the spleen in each group by FCM. (B) Apoptosis rates of CD4+ T cells from the spleen. Data are expressed as the mean ± standard error of the mean. **P<0.01 and *P<0.05. BSNXD, Bu-Shen-Ning-Xin Decoction; OVX, ovariectomized; E2, estradiol; FCM, flow cytometry; CD, cluster of differentiation.

T cells in OVX mice and the influence of BSNXD-derived serum, CD4+ T cells isolated from the spleen were divided into three groups for further analysis. One group was used to estimate the relative mRNA expression of RANKL and OPG by RT-qPCR. The second group was used to determine the cell surface expression of RANKL by FCM. The last group was cultured *in vitro* for 3 days, prior to harvesting of the supernatant to quantify soluble RANKL and OPG by ELISA. In the T cells from OVX mice a significant reduction in the expression of OPG mRNA was detected (P<0.01; Fig. 3A), and the expression of RANKL was significantly increased relative to that in the sham group mice (P<0.01; Fig. 3B). Those changes in mRNA expression were prevented with mid- and high-dose BSNXD and E2 treatment. In addition, low-dose BSNXD administration significantly increased the relative mRNA expression of OPG compared with that in the OVX group (P<0.01; Fig. 3A). Mid-dose BSNXD and E2 administration significantly alleviated the sharp increase in the cell surface expression of RANKL compared with that in the OVX group (P<0.01; Fig. 3C). The secretion of sRANKL by the CD4+ T cells was significantly increased in the OVX group compared with the sham group, and this increase was significantly inhibited by mid-dose BSNXD administration (P<0.01; Fig. 3D). The secreted OPG level of CD4+ T cells was significantly decreased in OVX group compared with the sham group (P<0.01; Fig. 3E). This reduction of OPG secretion was significantly attenuated in the OVX + mid-dose BSNXD-treated, OVX + E2-treated (P<0.01; Fig. 3E) and OVX + high-dose BSNXD-treated mice (P<0.05; Fig. 3E). Consideration of all these data led suggest that the treatment with BSNXD-derived serum ameliorated the imbalance of RANKL/OPG by downregulating the transcription, translation and cell-surface expression of RANKL and upregulating the transcription and translation of OPG in the CD4+ T cells of OVX mice.

*BSNXD inhibits CD4+ T cell-induced osteoclastogenesis.* Previous studies conducted by the present research team support the hypothesis that BSNXD markedly inhibits osteoclastogenesis by abrogation of RANKL-induced signaling pathways (34), and the present study indicates that BSNXD effectively suppresses OVX-induced expansion of the CD4+ T cell subset. Therefore, it appears that CD4+ T cells may be involved in the modulation of osteoclastogenesis by BSNXD. Accordingly, in order to investigate the effect of BSNXD on CD4+ T cell-induced osteoclastogenesis, CD4+ T cells from the spleen of mice were exposed to serial concentration (10, 15 and 20%) serum derived from OVX mice treated with BSNXD or E2 (containing 10 nM 17-β-estradiol) for 72 h and the apoptosis rate was mearsued by FCM. Results showed that with 15 and 20% serum treatment, the apoptosis rate of CD4+ T cells was decreased and the same effect can be observed by E2 treatment (Fig. 4, P<0.05, P<0.01 and P<0.01 respectively). BMMs from OVX mice were co-cultured with CD4+ T cells from OVX mice and exposed to 20% blood serum derived from untreated OVX mice, or OVX mice treated with mid-dose BSNXD or E2 for 72 h. BMMs cultured with 20% OVX group serum were considered as the negative control. These cells were fixed and subjected to TRAP staining. TRAP-positive MNCs containing five or more nuclei were counted as OCs (Fig. 5A). The results indicated that

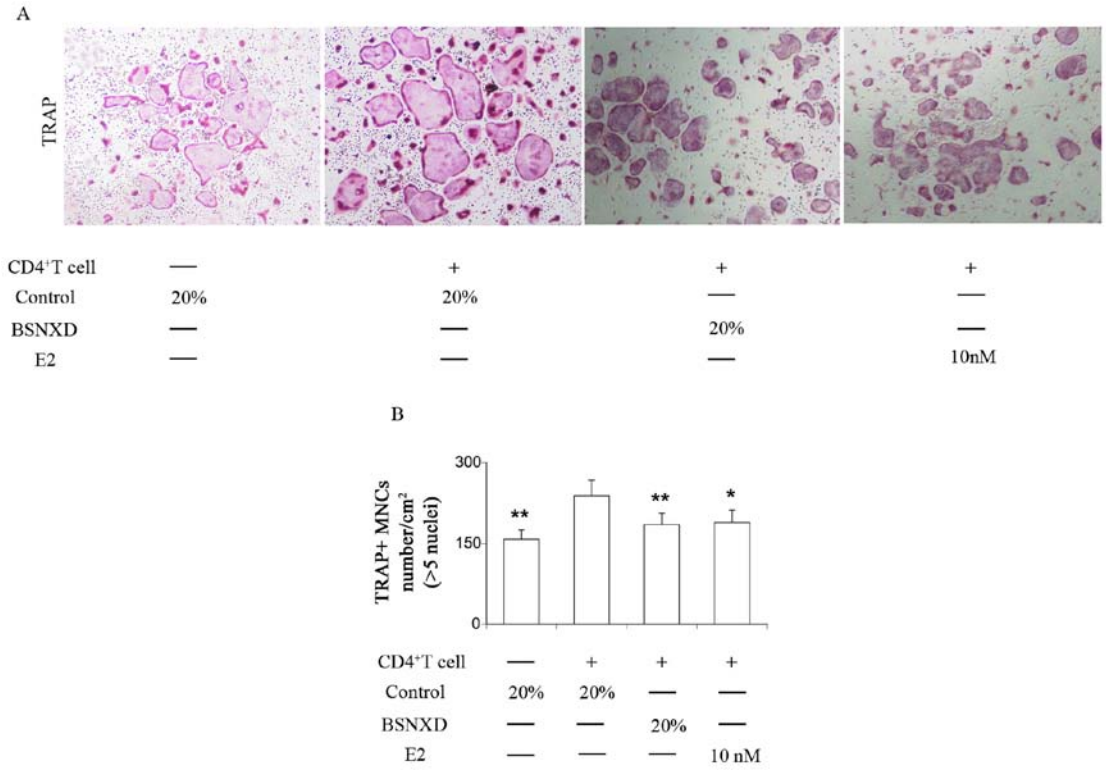


Figure 5. Effects of BSNXD administration on CD4+ T cell-induced osteoclastogenesis. BMMs from OVX mice were co-cultured with CD4+ T cells from OVX mice for 2 days in the presence of M-CSF and then exposed to 20% OVX + mid-dose BSNXD group-derived serum or OVX + E2 group-derived serum (containing 10 nM 17β-E2) independently plus M-CSF and RANKL for 3 days. BMMs cultured with 20% OVX group serum were considered as the negative control. Subsequently, the cells were fixed and stained for TRAP. TRAP-positive multinucleated cells containing five or more nuclei were counted as osteoclasts. (A) Representative images of the TRAP-positive MNCs in each groups. (B) TRAP-positive MNCs (more than five nuclei) were counted under a microscope. Data are expressed as the mean ± standard error of the mean. $^{**}$P<0.01. $^{*}$P<0.05. BMMs, bone marrow-derived macrophages; OVX, ovariectomized; BSNXD, Bu-Shen-Ning-Xin Decoction; E2, estradiol; TRAP, tartrate-resistant acid phosphatase; MNCs, multinucleated cells; M-CSF, macrophage-colony-stimulating factor; CD, cluster of differentiation.

TRAP-positive MNCs were significantly increased in number when co-cultured with CD4+ T cells from OVX mice, which indicates the involvement of CD4+ T cells in osteoclastogenesis in OVX mice (P<0.01; Fig. 5B). Treatment of OVX mice with BSNXD-treated mouse serum or E2 significantly inhibited the number of TRAP-positive MNCs, which indicates that CD4+ T cell-induced osteoclastogenesis was inhibited by BSNXD or E2 treatment (P<0.01 and P<0.05, respectively; Fig. 5B).

## Discussion

It has gradually been recognized that bones and the immune system mutually regulate each other to a much greater degree than was previously believed. The interdisciplinary research principle, which is known as osteoimmunology, mainly concentrates on the cross-talk between the bone and immune systems (9,12). PMO is a state of estrogen deficiency and a disordered state of bone metabolism, which involves the upregulation of osteoblast-mediated bone formation and OC-mediated bone resorption (41-43). However, the increased bone turnover shifts the bone homeostasis toward bone resorption. It also has been associated with various disorders of endocrine and immune origin (11,13,14).

The OVX mouse, serving as an animal mode of PMO, demonstrated an expansion of the CD4+ T cell pool in the BM and spleen via prolongation of the lifespan of CD4+ T cells

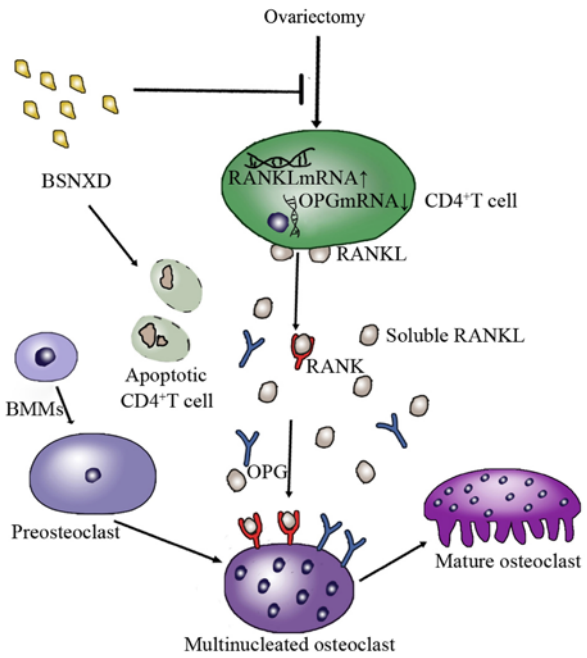


Figure 6. Summary of the CD4+ T cell-induced immunomodulatory effects of BSNXD on osteoclast differention. BSNXD suppresses ovariectomy-induced increases in CD4+ T cells subsets, adjusting the RANKL/OPG imbalance and the translation of these immunomodulatory effects on skeletal parameters such as osteoclastogenesis. BMMs, bone marrow-derived macrophages; BSNXD, Bu-Shen-Ning-Xin Decoction; RANKL, receptor activation of nuclear factor κB ligand-RANK, nuclear factor κB ligand; OPG, osteoprotegerin; CD, cluster of differentiation.

in the present study. In addition, it was also observed that BSNXD or E2 administration mitigated this OVX-induced expansion of $CD4^+$ T cells in the BM and spleen.

RANKL has been reported to serve an essential role in osteoclastogenesis; it is mainly expressed by stromal cells and osteoblasts, but T cells may also be a crucial source of RANKL in specific conditions such as PMO (44). $CD4^+$ T cells have the potential to adjust osteoclastogenesis bidirectionally by secreting pro-osteoclastogenic cytokines such as RANKL, as well as anti-osteoclastogenic cytokines such as OPG (45). The OPG/RANKL/RANK system is central to the coupling of OCs and osteoblasts in bone biology (46). Thus, the effect of BSNXD on OPG and RANKL mRNA transcription and expression in $CD4^+$ T cells was observed in the present study. The results demonstrated that $CD4^+$ T cells isolated from OVX mice and treated with BSNXD-derived serum exhibited increased levels of OPG mRNA and protein. Furthermore, BSNXD also reduced RANKL mRNA and protein levels, leading to a decreased RANKL/OPG ratio compared with that in OVX control mice. E2 administration exhibited a similar effect to that of BSNXD.

To assess whether RANKL secretion by T cells stimulates osteoclastogenesis, $CD4^+$ T cells were co-cultured with OC precursor cells and an increase in OC differentiation was observed. The results demonstrating that $CD4^+$ T cells promote osteoclastogenesis and BSNXD rebalances the OPG/RANKL/RANK system indicate that BSNXD has a positive effect on RANKL-induced osteoclastogenesis in BMMs *in vitro* and a negative effect on osteoclastogenesis (34). BSNXD administration also exhibited an ameliorating effect on the bone phenotype of OVX mice, which is in accordance with the hypothetical molecular mechanism suggested in the present study.

These observations indicate that an immune function disorder occurs in OVX mice. The results of the present study indicate that BSNXD reversed the detrimental immunological changes resulting from E2 deficiency and provided protection against bone loss. Based on these findings, it is proposed that BSNXD administration prevents bone loss by suppressing the OVX-induced expansion of $CD4^+$ T cells subsets and attenuating the imbalance of RANKL/OPG expression, and these immunomodulatory effects have subsequent effects on skeletal parameters such as osteoclastogenesis (Fig. 6), leading to an improved bone phenotype in mice.

Based on the beneficial effect of BSNXD administration on OVX mice that has been addressed previously (30,31,34), in association with the immunoprotective effect of BSNXD, the current findings appear to suggest that BSNXD provides skeletal preservation effects under estrogen deprivation. Therefore, it is proposed that BSNXD administration may have potential clinical value in the prophylaxis and therapy of PMO.

In conclusion, BSNXD, a herbal remedy used for centuries in TCM for the treatment of PMO, has previously been confirmed to have a bone protective effect in a mouse model for PMO. In the present study it was revealed that BSNXD has an immune-regulating effect on the bone phenotype of OVX mice by attenuating the reduced apoptosis rate of $CD4^+$ T cells, regulating the OVX-induced RANKL/OPG imbalance in $CD4^+$ T cells and attenuating osteoclastogenesis. This suggests that BSNXD may have potential clinical value as a prophylactic and therapeutic agent for PMO.

**Acknowledgements**

Not applicable.

**Funding**

The present study was supported by the National Natural Science Foundation of China (grant no. 31571196) to Ling Wang, the Science and Technology Commission of Shanghai Municipality 2015 YIXUEYINGDAO project (grant no. 15401932200) to Ling Wang, the FY2008 JSPS Postdoctoral Fellowship for Foreign Researchers P08471 to Ling Wang, the National Natural Science Foundation of China (grant no. 30801502) to Ling Wang, the Shanghai Pujiang Program (grant no. 11PJ1401900) to Ling Wang, the National Natural Science Foundation of China (grant no. 81401171) to Xue-Min Qiu, Development Project of Shanghai Peak Disciplines-Integrated Chinese and Western Medicine (grant no. 20150407) and the Program for Outstanding Medical Academic Leader to Da-Jin Li.

**Availability of data and materials**

All data generated or analyzed during this study are included in this published article.

**Authors contributions**

NZ was responsible for the feeding, surgery and drug administration of mice, XMQ performed the cell culture *in vitro*. WT and HJG provided technical support. DJL helped design this experiment. JLZ performed the real-time PCR, FCS and ELISA, and wrote the manuscript draft. LW was a major contributor in designing this study and writing the manuscript. All authors read and approved the final manuscript.

**Ethics approval and consent to participate**

The animal experiments were performed according to the Principles of Laboratory Animal Care of the Department of Laboratory Animal Science, Fudan University and approved by the Ethics Committee of Fudan University.

**Consent for publication**

Not applicable.

**Competing interests**

The authors declare that they have no competing interests.

**References**

1. Geusens P: New insights into treatment of osteoporosis in postmenopausal women. RMD open 1: e000051, 2015.
2. Recker R, Lappe J, Davies KM and Heaney R: Bone remodeling increases substantially in the years after menopause and remains increased in older osteoporosis patients. J Bone Miner Res 19: 1628-1633, 2004.
3. Bernabei R, Martone AM, Ortolani E, Landi F and Marzetti E: Screening, diagnosis and treatment of osteoporosis: a brief review. Clin Cases Miner Bone Metab 11: 201-207, 2014.

4. Danks L and Takayanagi H: Immunology and bone. J Biochem 154: 29-39, 2013.
5. Wada T, Nakashima T, Hiroshi N and Penninger JM: RANKL-RANK signaling in osteoclastogenesis and bone disease. Trends Mol Med 12: 17-25, 2006.
6. Leibbrandt A and Penninger JM: RANK(L) as a key target for controlling bone loss. Adv Exp Med Biol 647: 130-145, 2009.
7. Zhao P, Li J, Li Y, Tian Y, Wang Y and Zheng C: Systems pharmacology-based approach for dissecting the active ingredients and potential targets of the Chinese herbal Bufei Jianpi formula for the treatment of COPD. Int J Chron Obstruct Pulmon Dis 10: 2633-2656, 2015.
8. Penno H, Silfverswärd CJ, Frost A, Brändström H, Nilsson O and Ljunggren O: Osteoprotegerin secretion from prostate cancer is stimulated by cytokines, in vitro. Biochem Biophys Res Commun 293: 451-455, 2002.
9. Greenblatt MB and Shim JH: Osteoimmunology: A brief introduction. Immune Netw 13: 111-115, 2013.
10. Faienza MF, Ventura A, Marzano F and Cavallo L: Postmenopausal osteoporosis: The role of immune system cells. Clin Dev Immunol 2013: 575936, 2013.
11. Pacifici R: Estrogen deficiency, T cells and bone loss. Cell Immunol 252: 68-80, 2008.
12. Zhao R: Immune regulation of osteoclast function in postmenopausal osteoporosis: A critical interdisciplinary perspective. Int J Med Sci 9: 825-832, 2012.
13. Cenci S, Weitzmann MN, Roggia C, Namba N, Novack D, Woodring J and Pacifici R: Estrogen deficiency induces bone loss by enhancing T-cell production of TNF-alpha. J Clin Invest 106: 1229-1237, 2000.
14. D'Amelio P, Grimaldi A, Di Bella S, Brianza SZ, Cristofaro MA, Tamone C, Giribaldi G, Ulliers D, Pescarmona GP and Isaia G: Estrogen deficiency increases osteoclastogenesis up-regulating T cells activity: A key mechanism in osteoporosis. Bone 43: 92-100, 2008.
15. Sato K and Takayanagi H: Osteoclasts, rheumatoid arthritis and osteoimmunology. Curr Opin Rheumatol 18: 419-426, 2006.
16. Kong YY, Feige U, Sarosi I, Bolon B, Tafuri A, Morony S, Capparelli C, Li J, Elliott R, McCabe S, *et al*: Activated T cells regulate bone loss and joint destruction in adjuvant arthritis through osteoprotegerin ligand. Nature 402: 304-309, 1999.
17. Horwood NJ, Kartsogiannis V, Quinn JM, Romas E, Martin TJ and Gillespie MT: Activated T lymphocytes support osteoclast formation in vitro. Biochem Biophys Res Commun 265: 144-150, 1999.
18. Kotake S, Udagawa N, Hakoda M, Mogi M, Yano K, Tsuda E, Takahashi K, Furuya T, Ishiyama S, Kim KJ, *et al*: Activated human T cells directly induce osteoclastogenesis from human monocytes: Possible role of T cells in bone destruction in rheumatoid arthritis patients. Arthritis Rheum 44: 1003-1012, 2001.
19. Weitzmann MN, Cenci S, Rifas L, Haug J, Dipersio J and Pacifici R: T cell activation induces human osteoclast formation via receptor activator of nuclear factor kappaB ligand-dependent and -independent mechanisms. J Bone Miner Res 16: 328-337, 2001.
20. Wang R, Zhang L, Zhang X, Moreno J, Celluzzi C, Tondravi M and Shi Y: Regulation of activation-induced receptor activator of NF-kappaB ligand (RANKL) expression in T cells. Eur J Immunol 32: 1090-1098, 2002.
21. Maki PM: Critical window hypothesis of hormone therapy and cognition: a scientific update on clinical studies. Menopause 20: 695-709, 2013.
22. Hodis HN and Mack WJ: Hormone replacement therapy and the association with coronary heart disease and overall mortality: Clinical application of the timing hypothesis. J Steroid Biochem Mol Biol 142: 68-75, 2014.
23. López-Grueso R, Gambini J, Abdelaziz KM, Monleón D, Díaz A, El Alami M, Bonet-Costa V, Borrás C, Viña J, *et al*: Early, but not late onset estrogen replacement therapy prevents oxidative stress and metabolic alterations caused by ovariectomy. Antioxid Redox Signal 20: 236-246, 2014.
24. Russell RG, Watts NB, Ebetino FH and Rogers MJ: Mechanisms of action of bisphosphonates: similarities and differences and their potential influence on clinical efficacy. Osteoporos Int 19: 733-759, 2008.
25. Cummings SR, San Martin J, McClung MR, et al: Denosumab for prevention of fractures in postmenopausal women with osteoporosis. New Engl J Med 361: 756-765, 2009.
26. McCloskey EV, Johansson H, Oden A, et al: Denosumab reduces the risk of osteoporotic fractures in postmenopausal women, particularly in those with moderate to high fracture risk as assessed with FRAX. J Bone Min Res 27: 1480-1486, 2012.
27. Andreopoulou P and Bockman RS: Management of postmenopausal osteoporosis. Annu Rev Med 66: 329-342, 2015.
28. Wang L, Qiu XM, Hao Q and Li DJ: Anti-inflammatory effects of a Chinese herbal medicine in atherosclerosis via estrogen receptor β mediating nitric oxide production and NF-κB suppression in endothelial cells. Cell Death Dis 4: e551, 2013.
29. Wang L, Zhou GB, Liu P, Song JH, Liang Y, Yan XJ, Xu F, Wang BS, Mao JH, Shen ZX, *et al*: Dissection of mechanisms of Chinese medicinal formula Realgar-Indigo naturalis as an effective treatment for promyelocytic leukemia. Proc Natl Acad Sci USA 105: 4826-4831, 2008.
30. Wang L, Qiu XM, Gui YY, Xu YP, Gober HJ and Li DJ: Bu-Shen-Ning-Xin Decoction ameliorated the osteoporotic phenotype of ovariectomized mice without affecting the serum estrogen concentration or uterus. Drug Des Devel Ther 9: 5019-5031, 2015.
31. Gui Y, Qiu X, Xu Y, Li D and Wang L: Bu-Shen-Ning-Xin decoction suppresses osteoclastogenesis via increasing dehydroepiandrosterone to prevent postmenopausal osteoporosis. Biosci Trends 9: 169-181, 2015.
32. Nguyen K, Sparks J and Omoruyi FO: Investigation of the cytotoxicity, antioxidative and immune-modulatory effects of Ligusticum porteri (Osha) root extract on human peripheral blood lymphocytes. J Integr Med 14: 465-472, 2016.
33. Han BH, Lee YJ, Yoon JJ, Choi ES, Namgung S, Jin XJ, Jeong DH, Kang DG and Lee HS: Hwangryunhaedoktang exerts anti-inflammation on LPS-induced NO production by suppressing MAPK and NF-κB activation in RAW264.7 macrophages. J Integr Med 15: 326-336, 2017.
34. Wang L, Qiu XM, Gui YY, Xu YP, Gober HJ and Li DJ: Bu-Shen-Ning-Xin decoction: Inhibition of osteoclastogenesis by abrogation of the RANKL-induced NFATc1 and NF-κB signaling pathways via selective estrogen receptor α. Drug Des Devel Ther 9: 3755-3766, 2015.
35. Wang Y, Cui K, Zhao H, Li D, Wang W and Zhu Y: Bushen Ningxin Decoction pharmacological serum promotes the proliferation and suppresses the apoptosis of murine osteoblasts through MAPK pathway. J Ethnopharmacol 122: 221-226, 2009.
36. Wang L, Wang YD, Wang WJ and Li DJ: Differential regulation of dehydroepiandrosterone and estrogen on bone and uterus in ovariectomized mice. Osteoporos Int 20: 79-92, 2009.
37. Tyagi AM, Srivastava K, Kureel J, Kumar A, Raghuvanshi A, Yadav D, Maurya R, Goel A and Singh D: Premature T cell senescence in Ovx mice is inhibited by repletion of estrogen and medicarpin: a possible mechanism for alleviating bone loss. Osteoporos Int 23: 1151-1161, 2012.
38. Utermöhlen O, Tárnok A, Bönig L and Lehmann-Grube F: T lymphocyte-mediated antiviral immune responses in mice are diminished by treatment with monoclonal antibody directed against the interleukin-2 receptor. Eur J Immunol 24: 3093-3099, 1994.
39. Walsh NC, Alexander KA, Manning CA, Karmakar S, Wang JF, Weyand CM, Pettit AR and Gravallese EM: Activated human T cells express alternative mRNA transcripts encoding a secreted form of RANKL. Genes Immun 14: 336-345, 2013.
40. Senthilkumar R and Lee HW: CD137L- and RANKL-mediated reverse signals inhibit osteoclastogenesis and T lymphocyte proliferation. Immunobiology 214: 153-161, 2009.
41. Li JY, Tawfeek H, Bedi B, Yang X, Adams J, Gao KY, Zayzafoon M, Weitzmann MN and Pacifici R: Ovariectomy disregulates osteoblast and osteoclast formation through the T-cell receptor CD40 ligand. Proc Natl Acad Sci USA 108: 768-773, 2011.
42. Jilka RL, Hangoc G, Girasole G, Passeri G, Williams DC, Abrams JS, Boyce B, Broxmeyer H and Manolagas SC: Increased osteoclast development after estrogen loss: Mediation by interleukin-6. Science 257: 88-91, 1992.
43. Jilka RL, Takahashi K, Munshi M, Williams DC, Roberson PK and Manolagas SC: Loss of estrogen upregulates osteoblastogenesis in the murine bone marrow. Evidence for autonomy from factors released during bone resorption. J Clin Invest 101: 1942-1950, 1998.
44. Kim HR, Kim KW, Kim BM, Jung HG, Cho ML and Lee SH: Reciprocal activation of CD4+ T cells and synovial fibroblasts by stromal cell-derived factor 1 promotes RANKL expression and osteoclastogenesis in rheumatoid arthritis. Arthritis Rheumatol 66: 538-548, 2014.
45. Stein NC, Kreutzmann C, Zimmermann SP, Niebergall U, Hellmeyer L, Goettsch C, Schoppet M, Hofbauer LCl: Interleukin-4 and interleukin-13 stimulate the osteoclast inhibitor osteoprotegerin by human endothelial cells through the STAT6 pathway. J Bone Miner Res 23: 750-758, 2008.
46. Khosla S: Minireview: The OPG/RANKL/RANK system. Endocrinology 142: 5050-5055, 2001.